

Binding vs. scattering length: η in light nuclei

J.A. Niskanen^a H. Machner^b

^a*Department of Physics, PO Box 64, FIN-00014 University of Helsinki, Finland*

^b*Fachbereich Physik, Universität Duisburg-Essen, Lotharstr. 1, 47057 Duisburg, Germany*

Abstract

The possibility of etamesic nuclei remains an open problem in nuclear physics until now. Various calculations give contradictory predictions even for the lightest real nucleus ${}^3\text{He}$. In this paper we present the connection of the binding energy and width to the complex scattering length for s -states in heavier nuclei than this in the hope that, with knowledge of the final state interaction this could be useful in searches of possible bound states. It is seen that for a consistent analysis also the effective range should be considered.

Key words:

PACS: 12.38.Bx; 24.10.Ht; 13.60.Le

1 Introduction

In many unstable hadronic systems perhaps the only way to get information on their structure and interactions is the final state interaction in their formation process and associated decays, enhancement or decrease *vs.* free undistorted final state. Production slightly above the free threshold can yield also information on possible bound states below the threshold, especially if they are close to the threshold, *i.e.* weakly bound. This can be seen in the energy dependence [1,2] and described by the final state low-energy scattering parameters.

However, the cross section alone cannot distinguish whether the interaction can or cannot support a bound state. A textbook example is singlet S -wave NN scattering. It was necessary to indulge the difference in coherent neutron scattering off para- and orthohydrogen molecules to extract the sign of the large scattering length, which in turn showed that the interaction is not binding [3]. In most systems, in particular in case of spin-0 particles, this kind of

extra information is not available. However, as final state interaction analyses anyway give *some* information, it is conceivable that this would be useful in experimental searches for bound or quasibound states. In the latter case the problem can be far from trivial, since the state, even if "bound", can be wide and correspondingly the the low-energy scattering parameters would be complex.

An example of recent interest is the possibility of η -nuclear bound states. Numerous calculations exist, which disagree with each other completely especially for the lightest "real" nuclear systems with ${}^3\text{He}$ and ${}^4\text{He}$ [4–11]. Some of them indicate binding whereas most don't, while a general consensus is that by carbon binding should exist. Ref. [12] presents an overview of the confusion and a new fit for $(|a_R|, a_I)$ summarizing the experimental efforts.

Only a few experiments have been performed. One class of experiments produces the η -meson at rest in a quasi-free transfer reaction. In a second step the η interacts with a nucleon thus forming a resonance $N^*(1535)$ which can decay back to its entrance channel or, with 50% probability, into a nucleon and a pion. Since the η is at rest, these two final state particles are emitted almost back to back. The experiment by the GEM collaboration [13] claimed a 5σ effect in studying the $p+{}^{27}\text{Al}\rightarrow{}^3\text{He}+\pi^-+p+X$ reaction at a beam momentum for which the intermediate $X = \eta+(A-2)$ is almost at rest. In an experiment employing photoproduction the existence of η -mesic ${}^3\text{He}$ was claimed to have been observed in the reaction $\gamma+{}^3\text{He}\rightarrow\pi^0+p+X$ using the photon beam at MAMI [14]. Similarly as in the previous experiment a two step process was assumed but only the pion was measured and not the other nucleons. It has, however, been pointed out [15] on the basis of new high statistics data for the excitation function of the reaction $\gamma+{}^3\text{He}\rightarrow\pi^0+p+X$ that the data of Ref. [14] do not permit an unambiguous determination of the existence of a $\eta^3\text{He}$ -bound state, because nucleon resonances produce opening angle dependent structures in excitation functions and subtraction of excitation functions for different opening angles can produce artificial structures almost anywhere.

Inclusive experiments searching for η -mesic nuclei at BNL [16] and LAMPF [17] by using a missing-mass technique in the (π^+, p) reaction reached negative or inconclusive results. Later it became clear that the peaks are not necessarily narrow and that a better strategy of searching for η -nuclei is required as for instance applied in Ref. [13]. Furthermore, the BNL experiment was in a region far from the recoilless kinematics, so the cross section is substantially reduced [18].

Another class of experiments searched for η -mesic nuclei in final state interaction. Intensive studies were dedicated esp. to the $p+d\rightarrow\eta+{}^3\text{He}$ reaction [19–21]. The $\eta^4\text{He}$ final state has been studied in $d+d$ interactions making use of unpolarized beams [22–24] as well as polarized beams [25]. The very

large momentum transfer tends to make direct production of η mesons more difficult with larger nuclei. The heaviest system studied so far for final state interactions is $\eta^7\text{Be}$ produced in $p+^6\text{Li}$ reactions [26,27]. In this case there are only two data points at about 13 and 19 MeV above the threshold, so that no attempt for a final state interaction is possible, yet.

With reasonable assumptions of the Watson-Migdal theory [1, 2] final state studies can give estimates for the imaginary value of the scattering length and the absolute value of its real part [12]. However, the sign of the latter would be crucial as a tell-tale of a bound state. Still, even $|a_{\text{R}}|$ could give indications of the value of the binding energy, *provided it exists*, useful for experiments searching for such states. Further useful information would be expectations of the width of such states. The aim of the present paper is to continue to heavier light nuclei the investigation of Ref. [28] for ^3He on the relation between binding and the low-energy scattering parameters.

The paper presents the minute amount of formalism next and then the results for representative mass distributions of three light nuclei.

2 Formalism

There is not much actual new formalism in this paper. Rather the aim is a numerical extension of Ref. [28] to heavier nuclei than ^3He exposing more some details. The basic idea is to start from a simple optical model with a potential proportional to the density profile of the nucleus, use it to calculate the complex binding energy and scattering parameters separately and combine them to a common contour plot in the $(a_{\text{R}}, a_{\text{I}})$ plane. This presentation of the binding energy and width as a function of the complex scattering length is not necessarily trivial. However, due to the shape independence of nuclear forces with this phenomenology a connection between the basically distinct observables can be considered as better justified than their direct connection to the potential, independent on the validity of the simplest impulse approximation optical model.

For specificity (and to facilitate a comparison to the impulse approximation), the potential can be expressed as

$$V_{\text{opt}} = -4\pi(V_{\text{R}} + iV_{\text{I}})\rho(r)/(2\mu_{\eta N}), \quad (1)$$

with $\mu_{\eta N}$ the reduced mass of the ηN system. Here the nuclear density ρ can be varied from nucleus to nucleus and for each nucleus the strength parameters are freely varied to get a sufficient coverage of the $(a_{\text{R}}, a_{\text{I}})$ plane. It should be stressed that we are not predicting any absolute strength of the potential as in

the model works referred above. The main thing is the numerical connection of binding energies and widths to the scattering parameters, so that if the latter can be extracted from data, then a preliminary estimate could be obtained for the former. Although both are in some ranges sensitive to the potential parameters, in the spirit of the shape independence of NN forces, one might expect a relatively density profile independent connection. Indeed, in Ref. [28] it was checked that the relation between (V_R, V_I) and (a_R, a_I) was robust against changes in the density profile. In contrast to the free variation, within the optical model (as *e.g.* in Ref. [4]) the strength would be related to the elementary ηN scattering length as $V_{R(I)} = Aa_{\eta N, R(I)}$ with A the atomic number of the nucleus.

The scattering program is fairly standard even with a complex potential. This involves solving the Schrödinger equation with the proper asymptotic boundary condition

$$R_l(r) \sim j_l(kr + \delta_l) \quad (2)$$

with $k = \sqrt{2\mu_{\eta A}E/\hbar^2}$ and $\mu_{\eta A}$ is the reduced mass of the η -nuclear system. The binding solutions are obtained searching by iteration for poles in the homogeneous Lippmann-Schwinger integral equation (in configuration space)

$$R_l(r) = -ik \frac{2\mu_{\eta A}}{\hbar^2} \int_0^\infty j_l(kr_<) h_l^{(1)}(kr_>) V(r') R_l(r') r'^2 dr', \quad (3)$$

equivalent to the Schrödinger equation. The Green function arguments are $r_<$ ($r_>$) the smaller (larger) of r and r' . For s -wave bound states this reduces to

$$R_l(r) = -\kappa \frac{2\mu_{\eta A}}{\hbar^2} \int_0^\infty \frac{\sinh(\kappa r_<)}{\kappa r_<} \frac{\exp(\kappa r_>)}{\kappa r_>} V(r') R_l(r') r'^2 dr', \quad (4)$$

where now $\kappa = \sqrt{-2\mu_{\eta A}E/\hbar^2}$.

The convergence was good except for real potentials with very small binding energy (≤ 0.1 MeV) where the wave functions are much more extensive than the potential range. This case could reasonably be considered as essentially the zero binding limit with also extremely large cross section. Convergence stopped also in case of very large widths ($\Gamma/2 \geq 250$) MeV, in which case the wave functions tend to be of shorter range than the potential. The latter case is certainly not of experimental interest (with binding still at most in low tens of MeV or rather a few MeV).

The s -wave scattering parameters are defined as is standard for mesons by

$$q \cot \delta = \frac{1}{a} + \frac{1}{2} r_0 q^2 \quad (5)$$

so that for a real attractive potential $a_R < 0$ means binding (we shall later bring up a more exact condition). Experiments extract so far only the scattering length a , but it is notable that the effective range r_0 is of the same

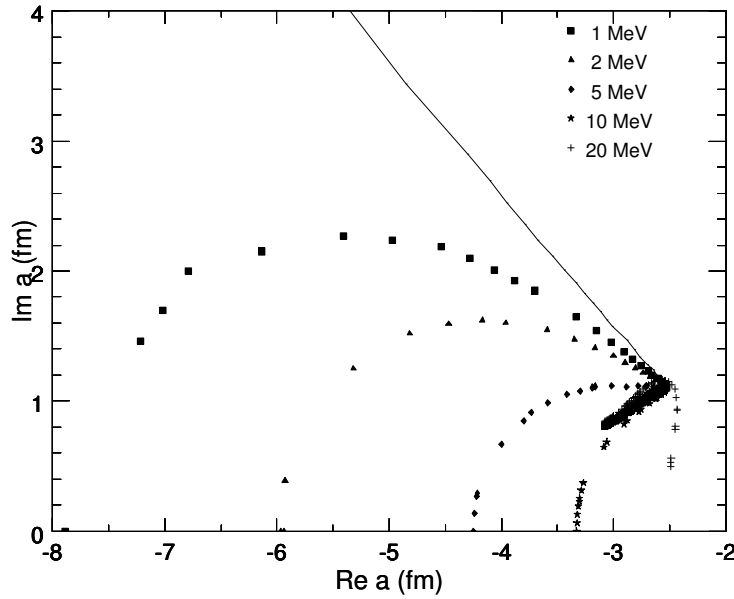


Fig. 1. The s -wave binding energy $E_B = -E_R$ contours for 1, 2, 5, 10 and 20 MeV in the complex (a_R, a_I) plane. The line shows the zero energy, *i.e.* above it there is no binding as explained in the text.

order in the range of most interest. Therefore, its experimental determination (or inclusion of theoretical predictions by hand) in analyses would also be of interest and importance.

3 Results

As a representative example the most detailed discussion is given to ^{12}C where binding is unanimously assumed. For this the modified harmonic oscillator of Ref. [29] is used as the density profile

$$\rho(r) = 0.17 \left[1 + 1.15 \left(\frac{r}{1.672} \right)^2 \right] \exp \left[-\left(r/1.672 \right)^2 \right] \text{ fm}^{-3} \quad (6)$$

with the normalization to the atomic number as $4\pi \int_0^\infty \rho r^2 dr = 12$ and r given in fm.

The basic results are given in Figs. 1 and 2, where the binding energies (defined as $E_B = -E_R > 0$) and half-widths $\Gamma/2 = -E_I$ are presented as contour points for 1, 2, 5, 10 and 20 MeV. The basic criterion for a printed point is that the deviation from the value is less than 0.05 MeV, though also a linear interpolation or extrapolation has been used in some more sensitive instances.

At least for real potentials and small binding in Fig. 1 the results follow well

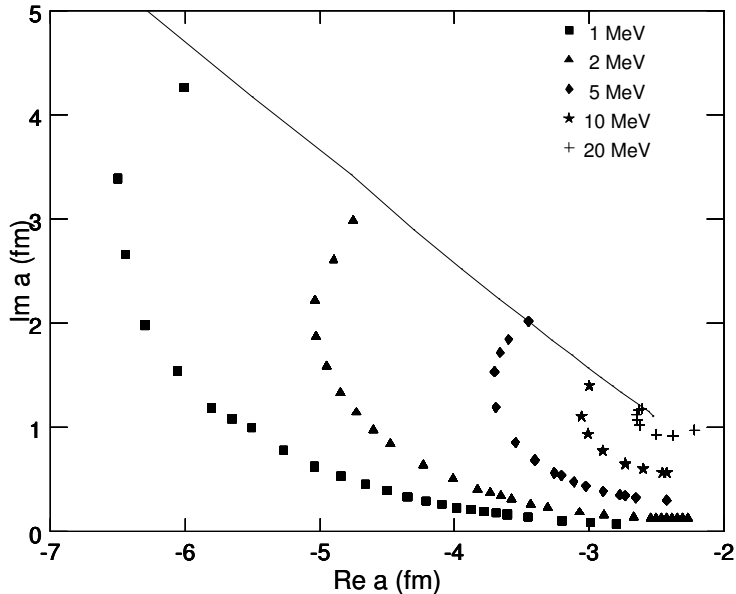


Fig. 2. The same as Fig. 1 but for the imaginary part of the bound state energies $-E_I$, *i.e.* half widths.

the trend $a \sim E_B^{-1/2}$ dictated by general arguments [30,31]. In fact, starting from the defining equation (5) one can derive a relation between the binding energy and low-energy parameters [32]. This can be generalized to the complex case as

$$1/a = -\sqrt{-2\mu_{\eta A} E/\hbar^2} - r_0 \mu_{\eta A} E/\hbar^2 \quad (7)$$

with $\mu_{\eta A}$ the reduced mass of the system. This relation was found to be amazingly accurate predicting the value of a well for binding energies up to $|E| \approx 10$ MeV and even beyond (a few percent for the real part and about ten percent for the imaginary; E and r_0 taken from the calculation). This success can be attributed to the inclusion of a non-zero effective range r_0 and can be considered as another indication of its importance.

Furthermore, it may be noted that for numerically bound points the condition [12]

$$\mathcal{R}[a^3(a^* - r_0^*)] > 0 \quad (8)$$

was well satisfied, while the simpler rule $|a_R| > a_I$ without the effective range, given *e.g.* in [11], extended for (wide) virtual states relatively far above threshold, *i.e.* the inequality was satisfied also for unbound states. This latter condition is equivalent to keeping only the first term in expression (8), so a comparison of the conditions is numerically possible. As seen in Fig. 3, also expression (8) could remain positive beyond the bound region, although it is mostly smaller, and both conditions decrease by an order of magnitude for decreasing E_R for each given V_R . Therefore, both conditions turn out to be necessary but not sufficient, though (8) is more precise. In fact, it also extends less to the

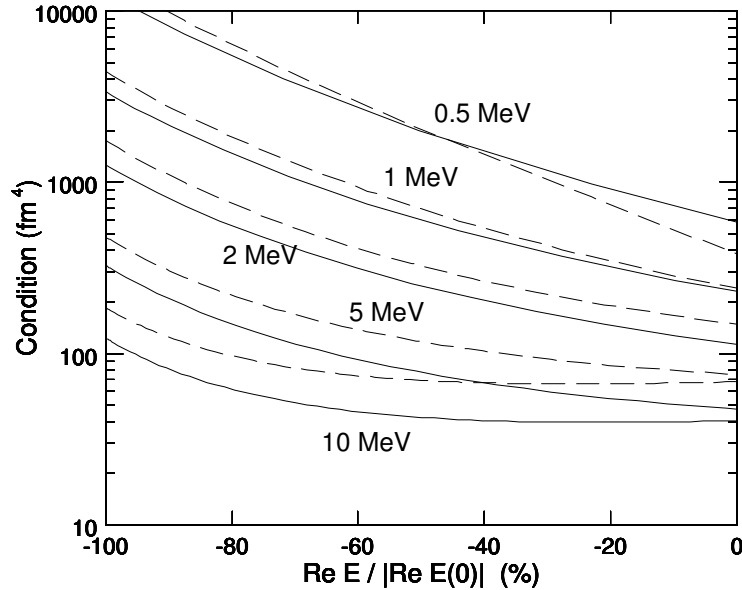


Fig. 3. The condition (8) (solid) *vs.* its first term (dashed) for five real potentials giving maximum binding energies indicated for real potentials. The horizontal axis is the percentage fraction $E_R(V_I)$ of $E_R(0)$.

unbound region.

With complex potentials the dependencies become nontrivial. As befits strong interactions, the strength of the potential V (real or imaginary) does not go to E or a linearly. However, in the former case the dependence of both E_R and E_I is anyway monotonous once the corresponding other part is kept constant. In contrast, for a given V_R a_I is *not* monotonous with respect to V_I . This behaviour results in the two "branches" of the E_R plots. The upper branch (starting from left for $E_R < 10$ MeV and potential real) could be considered as a "weak potential" part.¹ A general rule of thumb is that the imaginary potential, absorption, behaves like repulsion, although the above mentioned non-monotonousness means that, in a way as inelasticity, it eats its own effect out at some stage. While E_I grows with increasing V_I , the real part E_R decreases, eventually to no binding. This also means that for a given constant binding E_R a stronger V_R is needed, when V_I increases. In Fig. 1 the lower "strong potential" part is particularly dictated by the repulsive effect of the imaginary part of the potential. There an even mesh of potential strengths gives an increasingly dense accumulation of points. In this region a small change of the complex a (in particular a_I) can produce sizable changes

¹ It should be noted that this "branching" does not refer to the nomenclature in analyticity properties. Rather the question is about backbending of the curves. In the present results there is still a unique correspondence between the *complex* scattering lengths and energies.

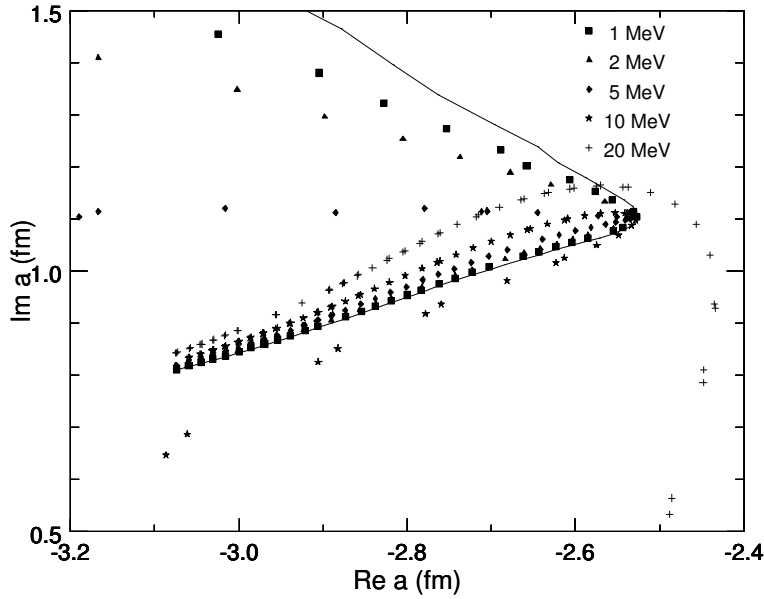


Fig. 4. Magnified detail of Fig. 1

in the binding and width. However, this region of $|a| \approx 2\text{--}3$ fm is also of most interest concerning both theoretical predictions and experiments at least in the helium case [12].

Therefore, Fig. 4 shows a magnified view of the backbending region. It can be seen that with increasing binding energy the upper "weak potential" branch comes down, whereas the lower "strong potential" part slowly bulges up. Therefore the opening angle between the weak and strong potential branches gets smaller until at about 9 MeV binding energy they switch over. Consequently, the zero binding curve (solid) in the lower branch is not actually a limit of possible bound states (as the upper branch of the solid line is). The "weak" coupling states get below it. It is also noteworthy that the strong coupling results as curves are not very far from each other (again in contrast to the weak coupling) and consequently not far from the lower zero energy line. In fact the 1 and 2 MeV results are indistinguishable in that case. Further it may be noted that the most "eastern" point of the zero binding curve is $(-2.525 + i 1.102)$ fm.

In addition to the absolute values of binding energies and widths, of paramount experimental interest is their relative magnitude. Typically for experimental recognition of a bound state one would hope the width or half-width to be less than the binding energy for distinguishing a state from continuum. For this purpose Fig. 5 shows by black points the region for which $|E_R| > |E_I|$. This belongs to the realm of "weak" coupling results. Quite clearly the real part of the scattering length in general should be larger than the imaginary part.

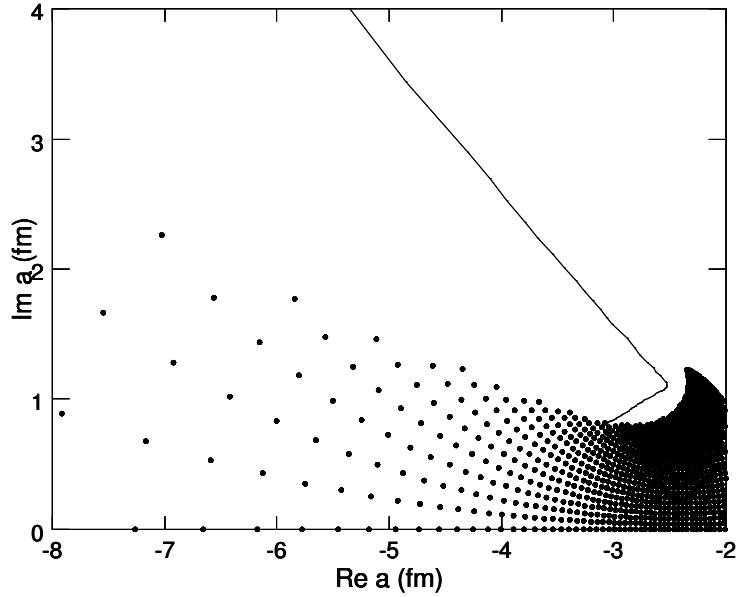


Fig. 5. The region where $|E_R| > |E_I|$. The solid curve is the zero binding limit.

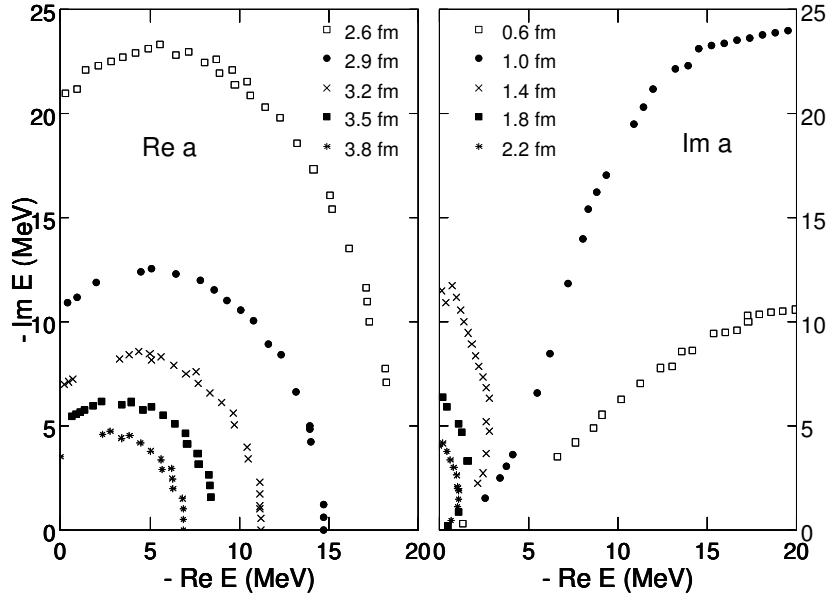


Fig. 6. The real and imaginary parts of the scattering length presented by contours in terms of the binding energy $E_B = -E_R$ and half-width $\Gamma/2 = -E_I$.

Sometimes it might be desired that possibly available binding energies would be used to predict or calculate as a test the low energy scattering parameters. Since without a too elaborate analysis or a detailed scattering calculation the effective range is not then known, a unique determination of the scattering length is not possible by Eq. (7) alone. Therefore, in Fig. 6 we give the reverted

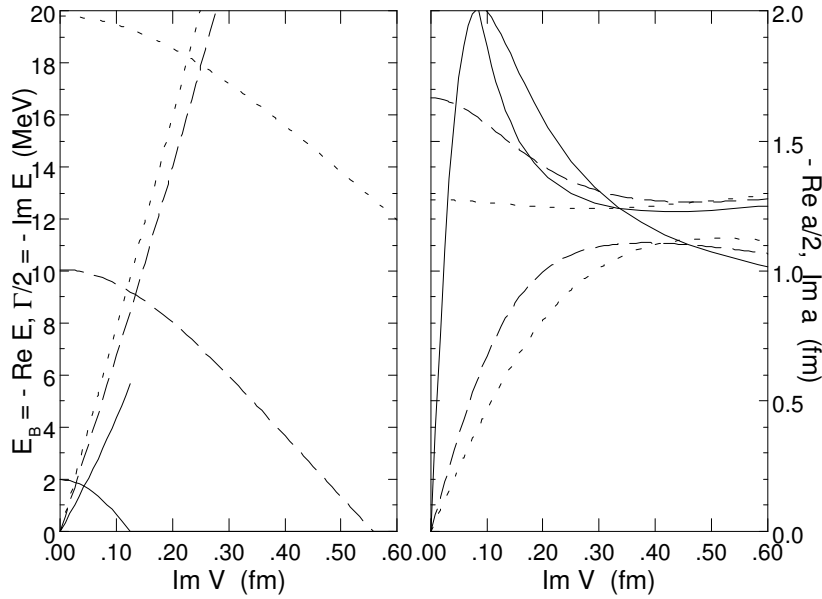


Fig. 7. Dependence of the s -state binding energies and half-widths (left panel) and the complex scattering lengths (right panel) on V_I . Three real potential strengths V_R are used, corresponding to binding energies of 2 (solid), 10 (dashed) and 20 MeV (dotted) in the real case, respectively, as explained in the text. The imaginary parts are curves starting from the origin, while the real parts start from finite values.

result for carbon, namely the components of the complex a as contours in the plane defined by the binding energy and half-width. Here the real part of the scattering length has double-valued relation to the width. Also a_I curves would return to the right side of the E_I axis for very large values of E_I , *i.e.* for width values above 100 MeV, clearly of no physical interest.

As the connection between the complex V and a clearly is not trivial, therefore, before going on to other nuclei it may be of interest to study their interdependence in some more detail, in particular the somewhat unintuitive effect of V_I . Along with the effect on the binding energy, this is done in Fig. 7, where these observables are shown as functions of V_I for three different values of V_R , which would give binding energies of 2 (solid), 10 (dashed) and 20 (dotted) MeV for the real case. These are obtained with V_R equal to 0.22, 0.37 and 0.50 fm, respectively, though, as stressed before, not too much weight should be associated with the absolute strengths of the phenomenological potential. However, these are provided here for reproducibility of the present results.

The binding energies $-E_R$ decrease fast with increasing V_I as expected (obviously starting from 2, 10 and 20 MeV for $V_I = 0$). The dependence of E_I on V_I is locally very well linear and steep. In the behaviour of the scattering lengths the first characteristic feature is the saturation of a_I , even turning slowly downwards, as mentioned earlier for the rising absorption potential

strength. (These curves are recognized as starting from the origin.) Further, the corresponding curves for $-a_R/2$ are shown. Also here the relative constancy of a_R is remarkable for the strongly imaginary potentials. The curves of the real part of the scattering length for all values of $V_R = 0$ appear to converge towards about -2.6 fm, apparently a sort of a "soft black sphere" limit. (It may be noted that the rms radius for this mass distribution is 2.44 fm.) These latter features cause the backbending of the constant energy curves and also the strong accumulation of points in Fig. 1. After all, it must be difficult to present E graphically as a function of nearly constant components of a . It is also worth noting that in the region of V_I where a_I reaches about 75 – 80% of its maximum and above, E_I (half-width) exceeds E_R .

Carbon in most models would support binding and it is also of great interest to get predictions for more controversial lighter nuclei with possible final state interaction fits. Therefore we used the three parameter Fermi distribution [29]

$$\rho(r) = 0.24 \frac{1 + 0.517r^2/0.964^2}{1 + \exp((r - 0.964)/0.322)} \text{ fm}^{-3} \quad (9)$$

for the density profile of ^4He to get similar estimates in a much lighter and more controversial case. ^3He was studied in Ref. [28] and the question raised again in Ref. [33]. Considering that even the nuclei are rather different, as seen in Fig. 8 the results are surprisingly similar to those of carbon. In practice only the turning point for weak and strong potentials has changed from about $(-2.5 + i 1.1)$ fm to $(-1.5 + i 0.9)$ fm. For a real potential the scattering length corresponding to 1 MeV binding changes from -7.9 fm to -7.4 fm. These, of course, reflect primarily the difference in effective ranges, which for carbon varies roughly between 2.5 fm ("weak" potential) and 1.5 fm ("strong") and for helium 1.7 fm and 1 fm, respectively, and is, of course, complex. With eq. (7) the differences would, thus, be as expected.

As an extension to heavier nuclei we choose to use also a three parameter Fermi distribution with $A = 24$ (^{24}Mg from Ref. ([29]))

$$\rho(r) = 0.17 \frac{1 - 0.163r^2/3.108^2}{1 + \exp((r - 3.108)/0.607)} \text{ fm}^{-3}. \quad (10)$$

This should be close enough a possible observation of a bound η state in ^{25}Mg of Ref. ([13]). The results for the binding energy contours are shown in Fig. 9. Especially up to the binding of 10 MeV they are very similar to those of carbon. Only this time the turning point has shifted to the left by about 0.6 fm. Taking the position of the minor peak of Ref. ([13]) below the $\eta^{25}\text{Mg}$ threshold for its face value as 13 MeV binding and estimating the half width from the data distribution to be 5 MeV would then correspond to the complex scattering length of $a \approx -3.1 + i 0.6$ fm (with also $r_0 \approx 1.6 - i 0.6$ fm; the calculated width and effective range not shown by figures). Now, if only one

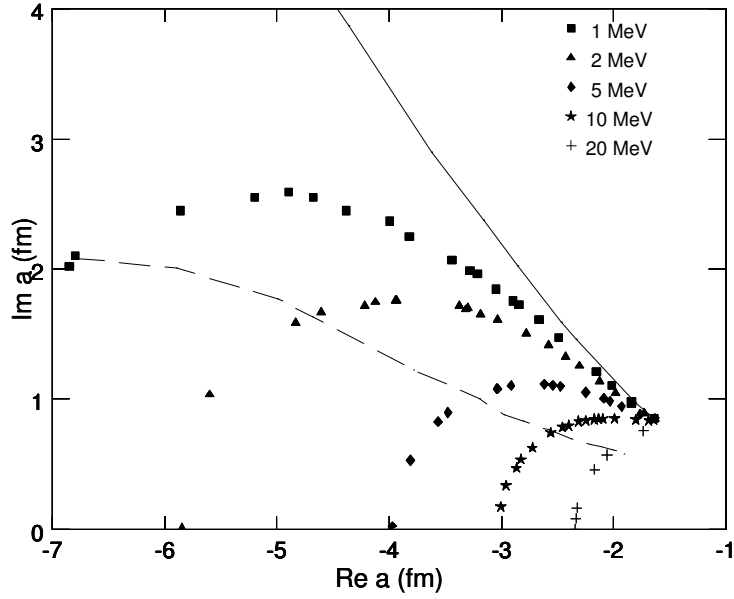


Fig. 8. The same as Fig. 1 but for the nucleus ${}^4\text{He}$. Below the dashed line $|E_R| > |E_I|$

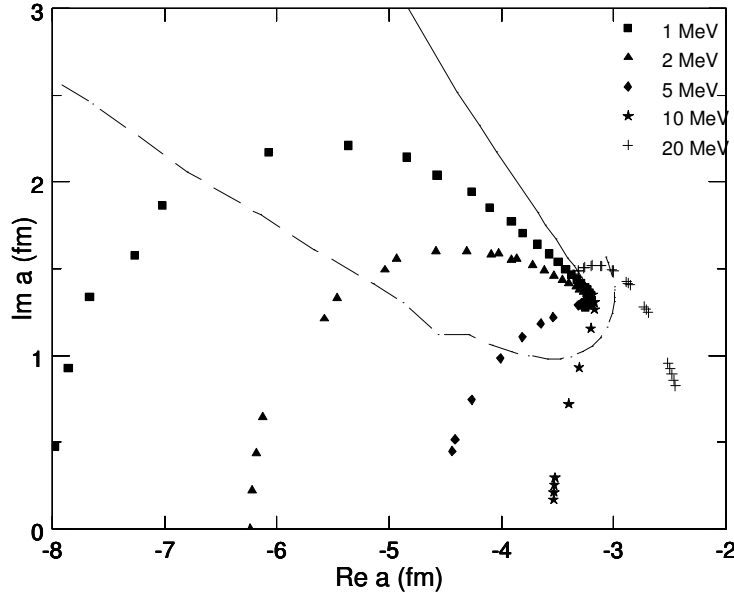


Fig. 9. The same as Fig. 1 but for the nucleus ${}^{24}\text{Mg}$. Below the dashed line $|E_R| > |E_I|$

had data on final state interactions in agreement with these, the additional data would corroborate the interpretation as a bound state.

From the figures 1, 8 and 9 one can see that for more extensive distributions of larger nuclei (increasing effective range) the energy contours shift to the left towards larger values of $|a|$. The same, of course, holds for inclusion or

exclusion of a positive effective range in analyses. This effect has actually been seen in analyses of Refs. [20, 21] for the $\eta^3\text{He}$ final state. Smyrski *et al.* get $a = [\pm(2.9 \pm 2.7) + i(3.2 \pm 1.8)]$ fm (without r_0), whereas Mersmann *et al.* quote a dramatically different value $a = [\pm(10.7 \pm 0.8_{-0.5}^{+0.1}) + i(1.5 \pm 2.6_{-0.9}^{+1.0})]$ fm (with r_0). One should note, however, that there is also a difference in taking into account the resolution smearing. Similarly Ref. [25] gives as the best fit $a = [\pm(3.1 \pm 0.5) + i(0 \pm 0.5)]$ fm without r_0 and $a = [\pm(6.2 \pm 1.9) + i(0.01 \pm 6.5)]$ fm with the effective range term included in the low energy expansion. Of course, these different results arise from the same physics, the same bound or unbound state. One may look at this effect also in another way. For the same values of a_R the binding energies should get bigger with a finite positive r_0 . So (assuming a negative a_R , *i.e.* a bound state) the first value of Ref. [25] would give a binding $E_B = 10 \pm 3$ MeV from Fig. 8 instead of 4 MeV without the second term in (7). However, the second value of a may be more consistent with reality, though one cannot say that from the fit itself. That would give a binding of about two MeV from Fig. 8.

So it seems likely that the effective range can be essential in a consistent analysis. In particular, a real first principles calculation for finite sized nuclei and the relation (7) cannot be accommodated without a finite r_0 and the same argument can be raised for data analyses. A single number for r_0 is not enough, since it is a function of the complex strength. Therefore, to facilitate its (at least approximate) use we give its real and imaginary components fitted as a second order bipolynomial form of the complex scattering length as

$$\text{Re } r_0 = c + d a_R + e a_I + f a_R^2 + g a_I^2 + h a_R a_I \quad (11)$$

and correspondingly for $\text{Im } r_0$, with the coefficients $c - h$ given in Table 1 for each nucleus and component. For numerical and physical reasons the fit was constrained to the regions $|a| < 8$ fm as in the figures, excluding the very large scattering lengths which would be inproportionately weighted by this form and for energies for which $|E_I| < |E_R|$ (the region of physical interest with distinguishable peaks). From the figures this would mean a binding of at least 1 MeV in the real case. Smaller binding might still be well described, since the second term in (7) should then become small. Discarding the excluded region improved the χ^2 significantly.

Thus all three observable quantities are interrelated. Once two are known, by shape independence quite well established in this work, the remaining one is determined without knowledge of actual potential details, such as its absolute strength. The moderate dependence on just the density profile may be a reasonable assumption as a starting point and could be taken from *e.g.* the present results.

Table 1

Coefficients of the powers or products of the expansion (11) for the complex effective range (a and r_0 in fm) for the three nuclei considered.

Quantity	Constant	a_R	a_I	a_R^2	a_I^2	$a_R a_I$
Re $r_0(^4\text{He})$	0.54215	-0.28931	0.11454	-0.015985	0.0041414	0.018879
Im $r_0(^4\text{He})$	0	0	-0.36374	0	-0.011609	-0.048794
Re $r_0(^{12}\text{C})$	-1.1515	-1.1416	0.30317	-0.090601	0.21724	0.10477
Im $r_0(^{12}\text{C})$	0	0	-1.207	0	-0.22788	-0.23799
Re $r_0(^{24}\text{Mg})$	-2.282	-1.5557	0.33591	-0.11709	0.26911	0.11353
Im $r_0(^{24}\text{Mg})$	0	0	-1.5419	0	-0.092067	-0.25479

4 Conclusion

In this work a phenomenological connection between the low energy scattering length and the complex binding energy of possible eta-nuclear bound states is studied in a simple but probably realistic model. The purpose of the work is that the results may be of use in searches of these bound states, if more easily accessible final state data are available to make predictions where to look for the states. The binding energies are explicitly presented as contours in the complex a plane for the nuclei ^{12}C , ^4He and ^{24}Mg . The well established and checked shape independence gives smooth systematics from which it is easy to interpolate and even extrapolate to other nuclei.

The calculations suggest that for even relatively moderate values of the imaginary potential and of the imaginary parts of the scattering lengths, the states can be wide especially compared with the real depths of the states. In view of also many other theoretical results, starting from the elementary ηN scattering and predicting negative real parts for the scattering length but with rather large imaginary parts, the observation of such bound states might be difficult or even impossible. However, in the minireview [12] of the situation a reanalysis of the existing data on $\eta^3\text{He}$ final states makes very small values of the imaginary part plausible, so that also the possible bound states may not necessarily be as wide as most theoretical works would indicate.

In our work for a_I less than 2 fm with a_R larger than, say, 5 fm a bound state should be recognizable. In the case of more likely smaller scattering lengths $a_I < 1$ fm would be necessary. In this respect the result $a_R = 6.2 \pm 1.9$ fm and $a_I = 0.001 \pm 6.5$ fm of Ref. [25] is quite interesting and suggestive. The relation between a and E (as discussed above and evidenced by Figs. 1, 8 and 9) is very robust against potential differences even between different nuclides over a wide range. Therefore, due to this shape independence one may trust

the results to be valid by interpolation also for the experimentally interesting $A = 7$ nuclei.

Acknowledgements

We thank Ch. Hanhart for useful discussions. This work was partly supported by the DAAD and Academy of Finland exchange programme projects 50740781 (Germany) and 139512 (Finland).

References

- [1] K.M. Watson, Phys. Rev. **88** (1952) 1163.
- [2] A.B. Migdal, JETP **1** (1955) 2.
- [3] J.M. Blatt and V.F. Weisskopf, Theoretical Nuclear Physics (Wiley, NY 1952).
- [4] C. Wilkin, Phys. Rev. C. **47** (1993) R938.
- [5] S. Wycech, A.M. Green and J.A. Niskanen, Phys. Rev. C **52** (1995) 544.
- [6] S.A. Rakityansky, S.A. Sofianos, M. Braun, V.B. Belyaev and W. Sandhas, Phys. Rev. C **53** (1996) R2043.
- [7] A. Fix and H. Arenhövel, Phys. Rev. C **66** (2002) 024002.
- [8] Q. Haider and L.C. Liu, Phys. Lett. B **172** (1986) 257.
- [9] L.C. Liu and Q. Haider, Phys. Rev. C **34** (1986) 1845.
- [10] H.C. Chiang, E. Oset and L.C. Liu, Phys. Rev. C **44** (1991) 738.
- [11] Q. Haider and L.C. Liu, Phys. Rev. C **66** (2002) 045208.
- [12] A. Sibirtsev, J. Haidenbauer, C. Hanhart, and J. A. Niskanen, Eur. Phys. Journal A **22** (2004) 495.
- [13] A. Budzanowski et al. (COSY-GEM collaboration), Phys. Rev. C **79** (2009) 012201R.
- [14] M. Pfeiffer et al., Phys. Rev. Lett. **92** (2004) 252001.
- [15] F. Pheron et al., Phys. Lett. B **709** (2012) 21.
- [16] R. E. Chrien et al., Phys. Rev. Lett., **60** (1988) 2595.
- [17] J. B. Lieb, *Proc. International Conf. Nuclear Physics, Sao Paulo, Sao Paulo, Brazil*, (1988).

- [18] H. Nagahiro, D. Jido, S. Hirenzaki, Phys. Rev. **C 80** (2009) 025205.
- [19] B. Mayer *et al.*, Phys. Rev. **C 53** (1996) 2068.
- [20] J. Smyrski, *et al.*, Phys. Lett. **B 649** (2007) 258.
- [21] T. Mersmann *et al.*, Phys. Rev. Lett. **98** (2007) 242301.
- [22] A. Wrońska *et al.*. The European Physical Journal **A 26** (2005) 421.
- [23] R. Frascaria *et al.*, Phys. Rev. **C 50** (1994) R537.
- [24] N. Willis *et al.*, Phys. Lett. **B 406** (1997) 14.
- [25] A. Budzanowski *et al.* (The GEM Collaboration) Nucl. Phys. **A 821** (2009) 193.
- [26] E. Scomparin *et al.*, J. Phys. **G 19** (1993) L51.
- [27] A. Budzanowski *et al.* (COSY-GEM collaboration), Phys. Rev. **C 82** (2010) 041001R.
- [28] A. Sibirtsev, J. Haidenbauer, J. A. Niskanen, and U. Meissner Phys. Rev. **C 70** (2004) 047001.
- [29] Atomic Data and Nuclear Data Tables, Vol. 14, No. 5,6, NOV/DEC 1974.
- [30] S. Weinberg, Phys. Rev. **131** (1963) 440.
- [31] V. Baru, J. Haidenbauer, C. Hanhart, Yu. Kalashnikova and A.E. Kudryatsev, Phys. Lett. **B 586** (2004) 53, [hep-ph/0308129].
- [32] Charles J. Joachain, Quantum Collision Theory, (North Holland, 1979), p. 291.
- [33] C. Wilkin *et al.*, Phys. Lett. **B** (2007) 92.